

College of Saint Benedict and Saint John's University

DigitalCommons@CSB/SJU

Celebrating Scholarship and Creativity Day
(2018-)

Undergraduate Research

5-4-2023

Transit Photometry of Multiple Exoplanet Watch Targets

Jonah Becken

College of Saint Benedict/Saint John's University, jbecken001@csbsju.edu

Follow this and additional works at: https://digitalcommons.csbsju.edu/ur_cscday



Part of the [Astrophysics and Astronomy Commons](#), and the [Physics Commons](#)

Recommended Citation

Becken, Jonah, "Transit Photometry of Multiple Exoplanet Watch Targets" (2023). *Celebrating Scholarship and Creativity Day (2018-)*. 228.

https://digitalcommons.csbsju.edu/ur_cscday/228

This Thesis is brought to you for free and open access by DigitalCommons@CSB/SJU. It has been accepted for inclusion in Celebrating Scholarship and Creativity Day (2018-) by an authorized administrator of DigitalCommons@CSB/SJU. For more information, please contact digitalcommons@csbsju.edu.

**TRANSIT PHOTOMETRY OF MULTIPLE EXOPLANET
WATCH TARGETS**

by

JONAH BECKEN

THESIS

Submitted in Partial Fulfillment of the
Requirements for the Degree of

**BACHELOR OF ARTS
PHYSICS**

College of Saint Benedicts & Saint John's University
St. Joseph/Collegeville, Minnesota

APRIL 2023

Transit Photometry of Multiple Exoplanet Watch Targets

Jonah Becken

College of Saint Benedicts & Saint John's University

Abstract

Since 1995 exoplanet research has increase dramatically, as a result it is more important than ever to precisely know the dates and times of future transits for repeated observations of a target. NASA's Exoplanet Watch database and accompanying light curve producing code EXOTIC have the goal of allowing small observatories across the world help find future transits. Under these objective observations of known exoplanet transits where made, using the Saint John's University observatory, to find the transit midpoint, the ratio of the planet radius and the solar radius, and the period. Using these values, the confirmation that a transit happened can be made, known periods may have their uncertainties reduced, and transit midpoints reported in BJD (Barycentric Julian Date) can be used to predict future transits most accurately. Additionally, the flat fielding done natively in EXOTIC was compared to an external custom flat fielding program to see if improvements in the above-mentioned values could be made. Of five observed transits two had midpoints that could be used for predicting future transits. The other values calculated had larger uncertainties than the current accepted values making them in significant. Comparisons of the native EXOTIC flat fielding and the external flat fielding showed that neither performed better, suggesting that there are improvements that could be made to EXOTIC.

Table of Contents

Table of Contents	3
List of Figures	5
List of Tables	6
1. Introduction	7
1.1 Why Observe Exoplanets?	7
1.2 Previous Work	7
1.3 Exoplanet Watch	8
1.4 EXOTIC Code and Possible Improvements	9
2. Materials & Methods	10
2.1 Experimental Setup	10
2.1.1 Image Capturing	10
2.1.2 Use and Setup of the CCD Sensor	12
2.2 Methods – EXOTIC	14
2.2.1 Flat-Fielding	14
2.2.2 Tracking the Star	15
2.2.3 Determining the Flux of the Target Star	16
2.2.4 Producing Light Curves	18
2.2.5 Problems with EXOTIC	19
2.2.6 Alternate Data Streams	20
3. Results	22
3.1 Overview of Results	22
3.2 Residuals and Transit Midpoints	23

3.3 Ratio of Exoplanet Radius to Stellar Radius	25
3.4 Exoplanet Periods	26
4. Conclusion	27
4.1 EXOTIC Flat Fielding vs. Pre-Flat Fielding	27
4.2 Midpoints and Radii Ratio	27
4.3 Exoplanet Orbital Periods	28
4.4 Future Works	28
References	29

List of Figures

Figure 1: Light Path Diagram of Meade LX200	11
Figure 2: CCD Linearity Plot	12
Figure 3: Photography Device's Quantum Efficiencies	13
Figure 4: Plots of X and Y Centroids	15
Figure 5: EXOTIC Aperture	16
Figure 6: Raw Flux to Normalized Flux	17
Figure 7: Plot of Airmass	18
Figure 8: Light Curve for HD 189733b	19
Figure 9: Data Stream Flow Chart	20
Figure 10: Light Curve for WASP-52b	22
Figure 11: Alternate Light Curve for WASP-52b	23
Figure 12: Light Curve for WASP-10b	25

List of Tables

Table 1: Star Residuals	24
Table 2: Transit Midpoints	24
Table 3: Observed R_p/R_s	26
Table 4: Observed Period	26

1. Introduction

1.1 Why Observe Exoplanets?

The discovery of exoplanets has been an important milestone in human achievement. As of 2023 over 5,000 exoplanets have been cataloged [1]. An exoplanet is a planet that orbits a star outside of the solar systems. Using telescopes and software exoplanet transits can be seen passing in front of their respective star or stars from earth. To see an exoplanet the intensity of the exoplanet's star is measured over a period of time and once there are a sufficient number of data points a light curve can be made which shows a dip in light intensity as the exoplanet passes in front of the star.

The study of exoplanets is motivated by two primary scientific interests. Firstly, scientists are interested in the possibility of finding another planet that can support life. The idea that we as humans are not alone has long captivated our imagination. Secondly, by studying exoplanets the origins of the creation of solar systems are able to be explored.

1.2 Pervious Work

Exoplanet research is a fledgling field, exoplanets were first discovered and confirmed in 1992 by Wolszczan and Frail [2]. The pair discovered multiple small planets orbiting a pulsar, using pulse signal timing. This discovery was followed by the multiple missions to find more exoplanets: NASA Kepler mission [3], K2 mission [4], and the Transiting Exoplanet Survey Satellite (TESS) mission [5]. Unlike Wolszczan's and Frail's discovery the previous three missions all used the transit method to discover exoplanets. Steve B. Howell outlined the challenges of exoplanet research and the motivations to pursue the research [6]. He outlines how

the field has broad research areas and appeal, the multi-disciplinary approach includes astronomy, astrobiology, biology, astrophysics, geology, and planetary sciences. On top of the satellite missions, he highlights the critical nature of ground based repeated observations of found exoplanets. In a culmination of the research and increased diverse interest and a statement that the field was established, exoplanet researchers Michel Mayor and Didier Queloz won the Nobel prize in 2019 for their discovery of the first exoplanet that wasn't orbiting a pulsar in 1995 [7].

Following observations of known exoplanets help researchers understand the orbital parameters, the planet's environment, and the planet's atmosphere. This information is used to unpack the origins of the universe, but also aid the search for life. In this search for life researchers are looking at found exoplanets to find those that have similar characteristics to Earth. In 2019 Howell made observations on a binary star system Kelper-13AB to determine which star Kelper-13b orbits [8]. Roughly 46 percent of exoplanets are in binary star systems and there are roughly 125 billion Earth like planets in our galaxy, meaning that nearly 60 billion Earth like planets are in binary systems. To support the search life, it is important to know which star the exoplanet orbits. Howell used multiple high-resolution observations to find the transit of Kelper-13b. Howell determined that Kelper-13b orbited star A in the binary system.

1.3 Exoplanet Watch

Exoplanet Watch is a database of exoplanet transits formed through a collaborative observation effort lead by NASA. The database allows independent observers to find exoplanet targets which they will have the ability to observe. The goal of Exoplanet Watch is to refine the transit of

known exoplanets through many observations. The database ranks each exoplanet, and the higher an exoplanet ranks the more desire there is for its transit to be refined.

There are many scientific advantages that motivate the creation and use of the Exoplanet Watch database. Through the refining of these exoplanet transits other larger observatories/telescopes, like James Webb or Hubble, are able to observe more targets. The transits also help with the discovery of new exoplanets by comparing variations in the known transits to infer the existence of new exoplanets. Another advantage is that stellar variability is able to be monitored as enough transits of exoplanets are collected. Lastly, exoplanet existences are able to be confirmed by the Exoplanet Watch database.

1.4 EXOTIC Code and Possible Improvements

EXOTIC is the data processing software provided by NASA's Exoplanet Watch and Caltech [9]. While the program is already well-designed aspects of it can be improved. Using an external flat fielding program and EXOTIC's own flat fielding, problems with EXOTIC's flat fielding can be revealed and the possible improvements can be made. By improving the EXOTIC software's native flat fielding, the objective of Exoplanet Watch can be better achieved.

2. Materials & Methods

2.1 Experimental Setup

2.1.1 Image Capturing

Firstly, a target exoplanet is selected by using Swarthmore College's Exoplanet Transit Finder tool [10]. Specifically, the only targets considered are part of the NASA Exoplanet Archive database target list option. This limits the targets to only those that the Exoplanet Watch project is interested in. Once a target has been selected the process of collecting images can begin.

Images were collected using a telescope on a tracking mount with a CCD camera attached to the telescope. The specific telescope used was a Meade LX200 12 inches made by Meade Instruments. The Meade LX200 has an aperture of 12 inches, a focal length of 3048mm, and has a resolving power of 0.380 arcseconds, see figure 1 [11]. Before images of the target are collected flats and darks are taken at varying time scales for later use/error correction when processing the raw data. The flats are collected while looking at a flat blue sky as the sun is setting, the objective to the flats is to capture images with the different filters while maintaining a light intensity around 50 to 60 percent of the maximum light intensity the CCD sensor can discern. Staying inside the CCD's range where it behaves linearly is important, figure 2 shows how a CCD starts to perform non-linearly as it nears saturation. The objective of the darks is for use in dark subtractions of the target images to reduce their error. Often the darks are taken again immediately after the target images are taken and then subsequently subtracted rendering the earlier darks unneeded; however, the initial darks are still taken in case the capture and subtraction of darks cannot be done synchronously with the target images.

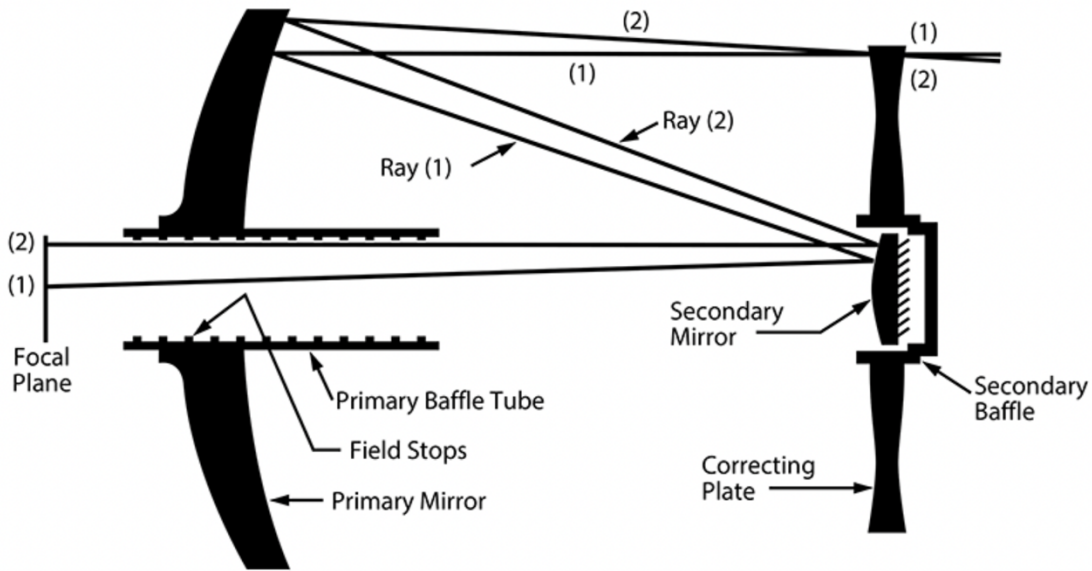


Figure 1 Shows a light ray's path through the Meade LX200 12-inch telescope. (1) and (2) are two different incident light rays [11].

After the darks and flats are taken the telescope must be focused. The focusing is achieved by observing a star of a magnitude that is similar to the target and maximizing the light intensity that the CCD can observe. The telescope and CCD are now ready to collect images of the target. Images are captured of the target making sure that the light intensity of the target stays at or above 20 percent of saturation for the CCD sensor. All image files (flats, darks, target images) are saved as a flexible image transport system (FITS) file.

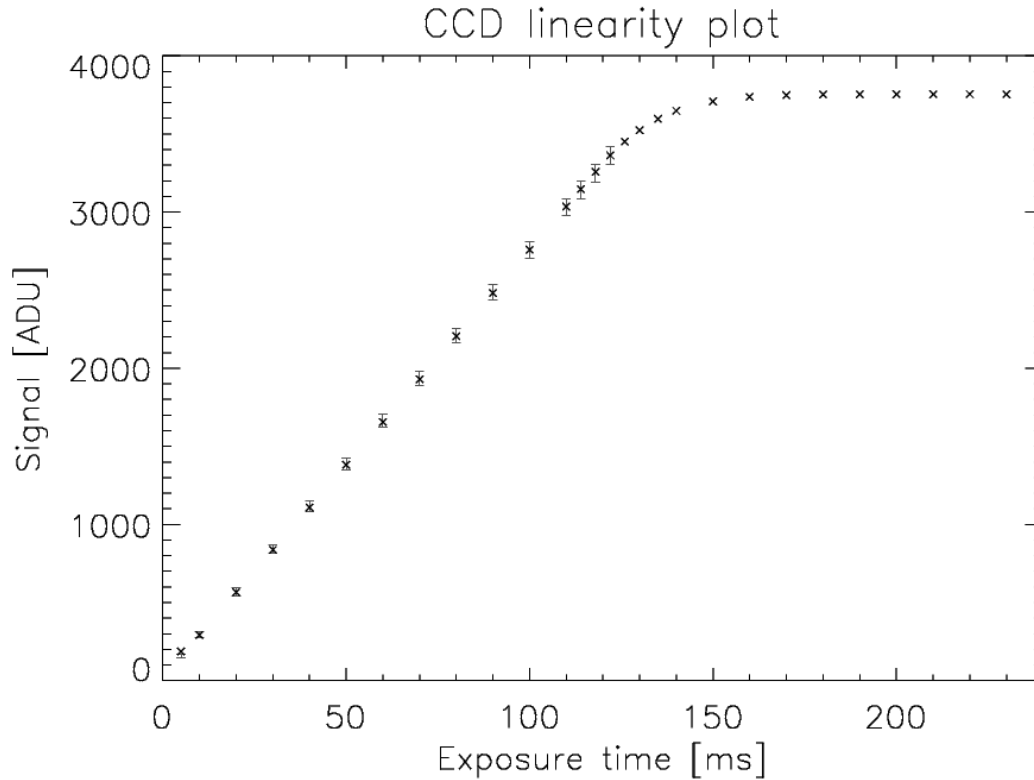


Figure 2 Plot shows how as the exposure time, and thus the saturation of the CCD, makes the signal non-linear as the saturation gets too high. Due to the non-linear nature, it is important to not overexpose the CCD sensor [12].

2.1.2 Use and Setup of the CCD Sensor

A CCD (charged-coupled device) sensor is an uncommon sensor for ordinary photography applications; however, its use in astronomical observations is quite common. A CCD sensor is made almost entirely of silicon, it consists of a number of wells/pixels that are each accompanied by a capacitor. The absorption length of silicon is 350 nm to 800 nm, and since a CCD is almost entirely silicon the same absorption length applies [13]. The main advantage of a using a CCD sensor is that it has a high quantum efficiency (QE) for certain wavelengths. This QE does vary in peak efficiency and wavelength for different configurations of CCD sensors, but still the overall QE is much higher than that of other electronic image capturing devices. In a CCD sensor the thickness of the sensor has a large impact on the QE, the thicker the sensor the larger the

wavelength that can be absorbed. Figure 3 below shows the QE of multiple CCD sensors and other photographic devices.

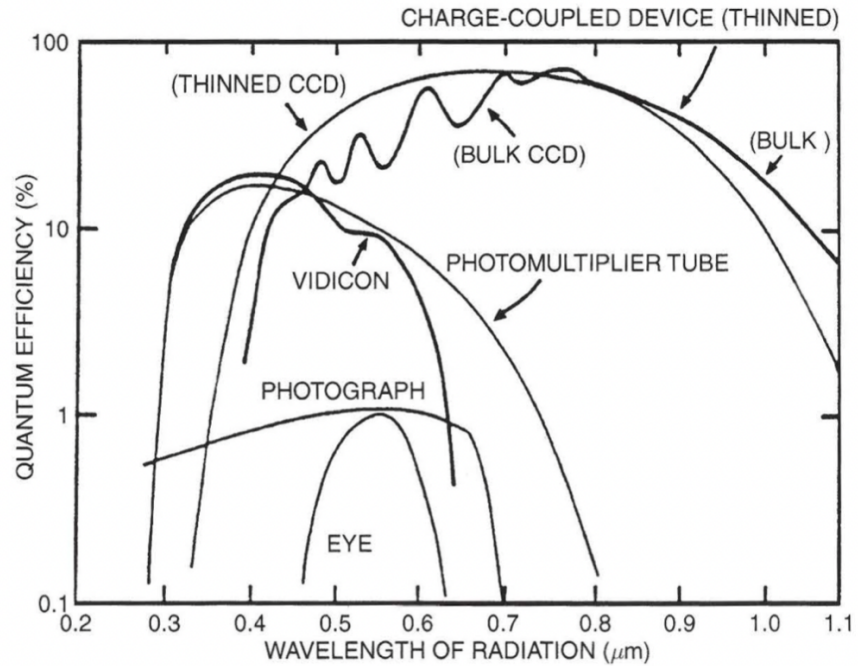


Figure 3 Plot shows different photography devices. It is evident from this plot that CCD's have a much higher QE compared to other devices. The plot also shows the different wavelengths that varying CCD types have [13].

When a CCD does a readout of an image it transfers the charge of each pixel out one at a time. This means that the transferring of the charge from pixel to pixel must be extremely efficient. Charge Transfer efficiency (CTE) is a measure of the fraction of charge that is transferred from one pixel to another [13]. The CTE of a typical CCD is around 0.999995. This is especially important when a sensor is that 2048 by 2048 pixels requires a charge to be transferred 4096 times. If the CTE is even 0.999 there will be considerable charge loss by the time the last pixel is readout.

Dark currents are another reality of CCDs, they appear when energy in the sensor creates thermal noise. The meaning of this is that when the thermal energy is high enough, electrons will be released from the valence band of the silicon and collected into the pixel wells [13]. The collection of electrons into the pixel wells are then registered as a light ray. Once read out the images will not have any mechanism to determine whether or not the intensity is from the dark current or from the target. In order to mitigate the effects of dark currents the CCD sensor is cooled down to a temperature around $-10\text{ }^{\circ}\text{C}$ to $-20\text{ }^{\circ}\text{C}$. By reducing the thermal energy of the sensor there will be less valence electrons collecting in the pixel wells and thus reducing the effects of the dark currents when the images are read out. Dark subtractions are still necessary, but the reduction in dark currents from sensor cooling are important since they allow the CCD to have a larger useable saturation limit.

2.2 Methods – EXOTIC

2.2.1 Flat-Fielding

The QE of a CCD is considered in theory to be the same for every pixel, in reality each pixel has a slightly different QE. In addition, flat fielding is used to remove optical imperfections that come from dust or scratches on the sensor cover and the telescope dust cover. This is what makes flat fielding a necessary step when processing the target images.

Flat fielding is achieved by dividing the pixel intensities of the images to be processed by the flat field image. To get the “master” flat field image used the median of a set of flat field images is found. Then the median of that set is found, after which the average of this image is found and then divided from the median of the set of flats. This results in the “master” flat which is used for

flat fielding the target images. The different approaches to flat fielding the images are discussed in depth in section 2.2.6.

2.2.2 Tracking the Star

The first step of EXOTIC's data processing pipeline is to find the target and then track the target throughout all of the images. In order to achieve this, it asks the user to input the pixel coordinates corresponding to the location of the target. It would be simple to keep this same pixel coordinate for each subsequent image; however, the position of the target within the frame is likely to change over the course the night so a routine to track the target is necessary.

Using the location of the target supplied by the user, a 2D Gaussian function or centroid is fitted to the image using least squares fit model to find the center of the target, see figure 4 [14]. In figure 3 below the plots of the x and y pixel positions for each image are shown, displaying the necessity for target tracking. Not only is the target tracked but the comparison stars are also tracked using the same process.

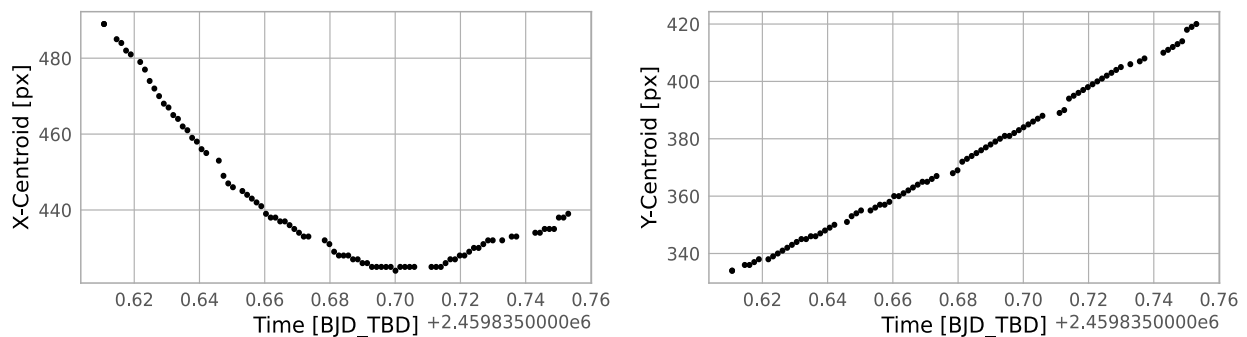


Figure 4 Plots of the x and y centroids for a comparison star observed on September 12th, 2022. If tracking were perfect both lines would be at a constant value. The importance of star tracking is revealed by the dramatic change in positions of near 100 pixels that are observed.

2.2.3 Determining the Flux of the Target Star

Once the tracking of the target and comparison stars has been established the program must determine the flux of the target. In order to compute the flux of the target a circular aperture extraction is performed by EXOTIC. Figure 5 depicts how the program views the star during the flux extraction process. The first step of the flux extraction requires the program to sum all the pixel values inside of the red aperture [14]. This sum is now the total amount of light detected within the red circle. It would be wrong to treat this total as the true amount of light detected from the star since it is impossible to know at this point what light is from the background and what light is truly from the target. In order to isolate just the light emitted by the star the pixel values from in-between the green and red circles are summed. Once summed the average value of those pixels is subtracted from each pixel within the red circle to give a raw flux of the star. This process is completed for both the target and comparison stars.

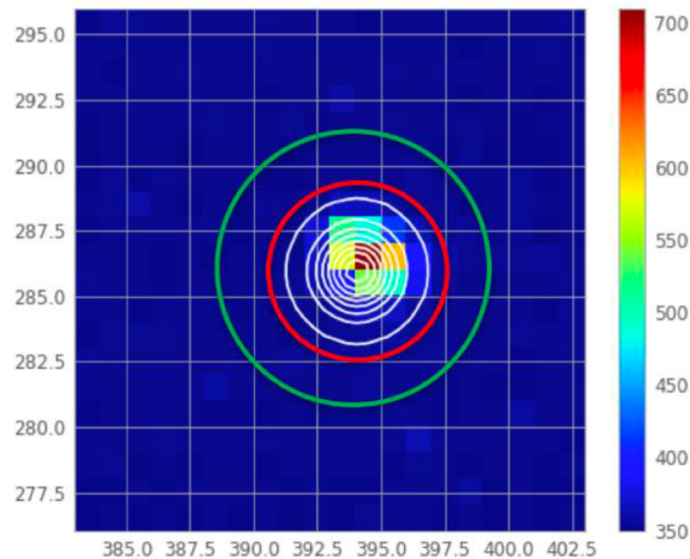


Figure 5 A subsection of an image from the EXOTIC literature looking at the exoplanet HAT-P-32b [14]. The red circle is the target aperture, and the green circle is used for calculations of background light. The white circles are used for the target tracking feature.

Once the raw flux of the target has been calculated the target’s flux needs to be normalized to correct for any sources of error. In order to make this correction the raw flux of a comparison star is calculated and then divided into the raw flux of the target [14]. Often multiple comparison stars are given to EXOTIC, and it chooses the best comparison star by fitting a model light curve developed by Gael Roudier [14]. The model is a simple least-squares fit. Whichever comparison star fits the model best is selected to be used for the rest of the data reduction process. This process results in the normalized flux of the target star, see figure 6. In theory the comparison star should have a constant flux value; however, this is not the case, and the flux does change over time. As can be seen in figure 6 though both the target and comparison star follow roughly the same non-constant path, and the points where they do not follow the same path is when the exoplanet is transiting the target star.

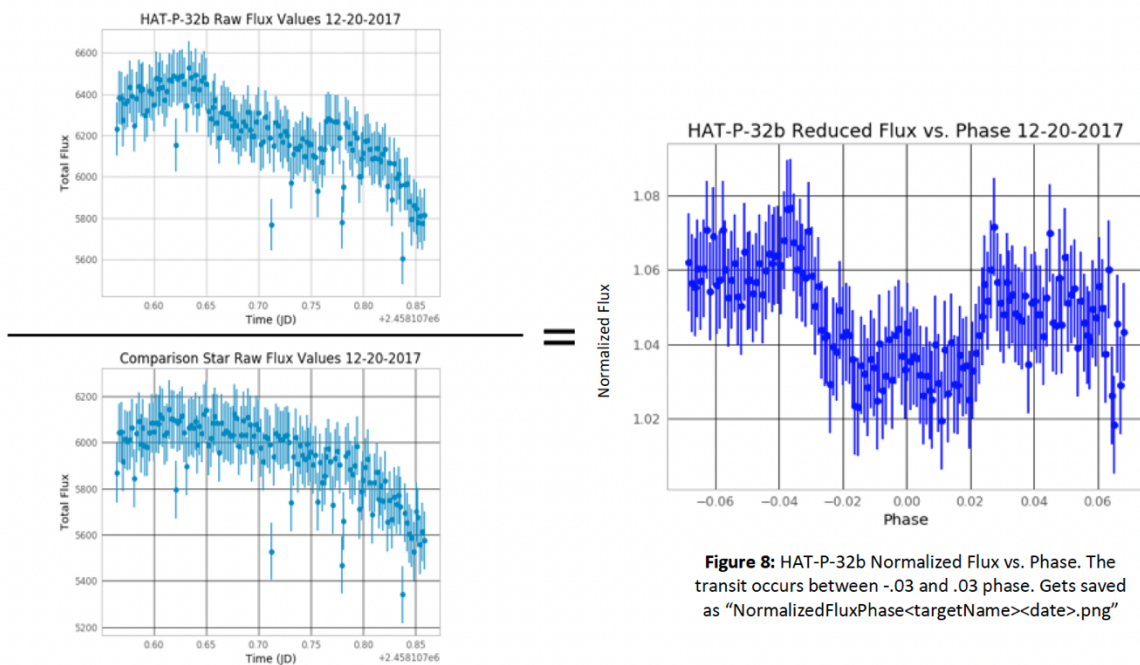


Figure 8: HAT-P-32b Normalized Flux vs. Phase. The transit occurs between -.03 and .03 phase. Gets saved as "NormalizedFluxPhase<targetName><date>.png"

Figure 6 The non-constant nature of both the comparison star and the target can be seen on the left side. Once the raw target flux is divided by the comparison star’s raw flux the normalized flux can be plotted as a function of the orbital phase. A phase of 0 corresponds to the exoplanet being directly in front of its star [14].

2.2.4 Producing Light Curves

Now that the images have been flat fielded, the target tracked, and the normalized flux found a light curve can be fit to the data set. The most important variables that affect the shape of the light curve are the ratio of the exoplanet's radius to its host star, the mid-transit time, and the orbital period [14]. The last two variables are especially important to Exoplanet Watch as they help determine when the exoplanet will be transiting its host star.

Unlike the least-squares fits used for tracking the target and determining the best comparison star, the light curve model uses a Monte-Carlo Markov Chain (MCMC) simulation. The MCMC is able to explore a larger range of possible fits to determine the best fit. In EXOTIC the MCMC fits for the mid-transit time and the ratio of the exoplanet's radius to its host star [14]. Since the amount of atmosphere that the telescope is looking through changes throughout the night coefficients A and B of the following airmass determined from the MCMC fit.

$$f = A \times e^{B \times \text{Airmass}} \quad (1)$$

Figures 7 and 8 shows the results of the MCMC fitting routine.

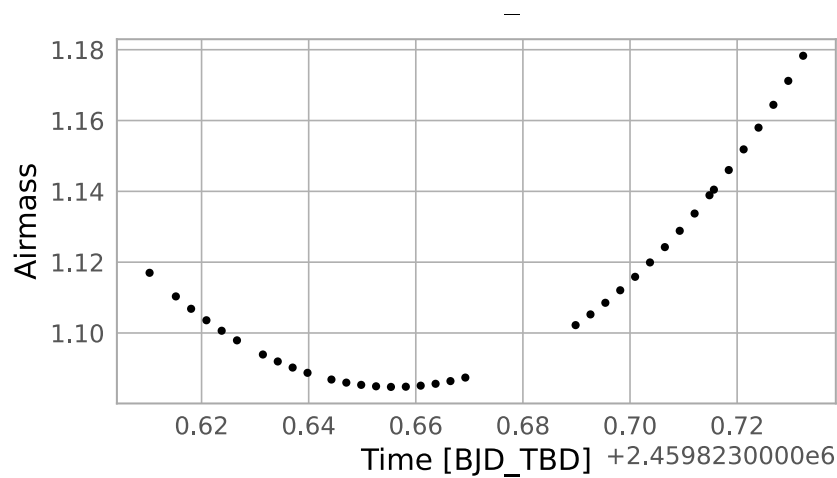


Figure 7 Plot of the change in airmass throughout the observation taken on September 12th, 2022. The airmass changes as the target is tracked across the sky and the amount of atmosphere being looked through changes.

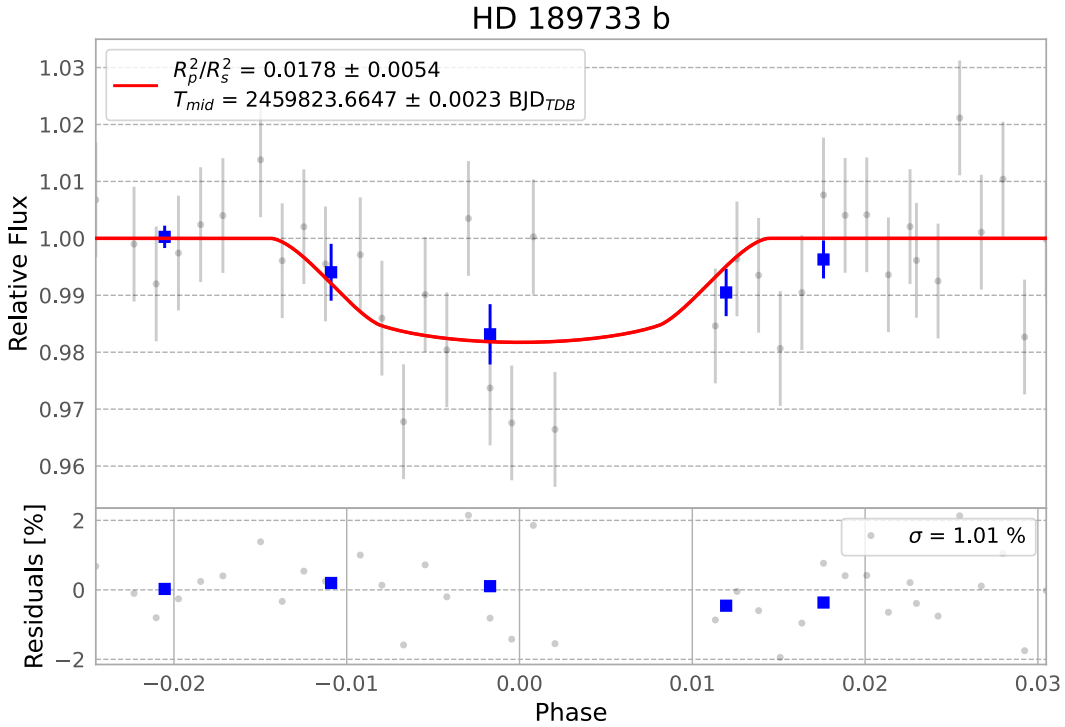


Figure 8 Results of EXOTIC MCMC fitting routine for the target HD189733b. The R_p^2/R_s^2 value corresponds to the transit depth, the T_{mid} value corresponds to the exact time of specific transits midpoint, and σ value corresponds to the residuals.

2.2.5 Problems with EXOTIC

While processing data with EXOTIC the effectiveness of the in-line flat fielding came into question. Some light curve results led to the hypothesis that prepose the flat fielding was not being completed effectively. The residuals in the final light curves were relatively high and the uncertainties in the ratios of radius was much larger than expected (uncertainties of the same magnitude as the results were observed). This issue was addressed by comparing pre-flat fielding images to EXOTIC and comparing to the flat fielding done natively by EXOTIC. Section 2.2.6 will discuss in more detail the differing data pipelines.

2.2.6 Alternate Data Streams

In order to test the flat fielding capabilities of EXOTIC two differing data pipelines were created. Each data set was processed through each pipeline and their results compared. Figure 9 displays the different pipelines the data traveled through.

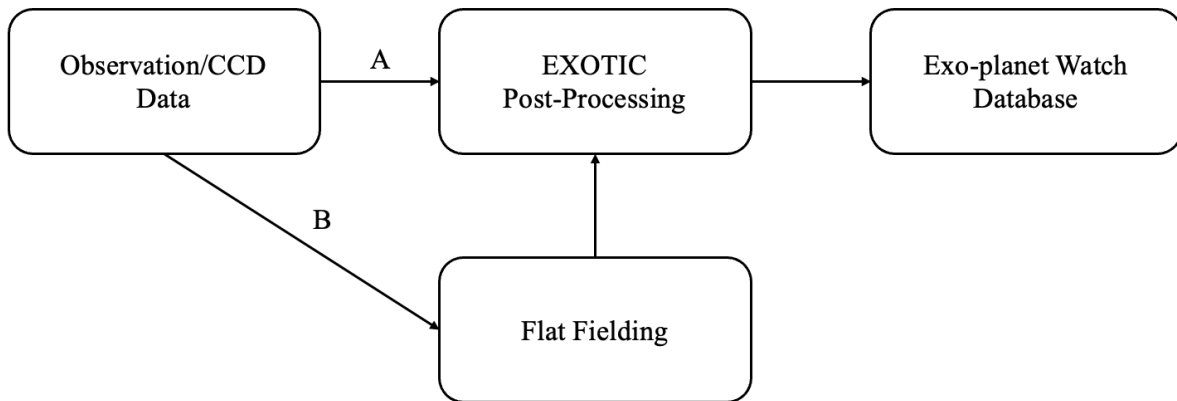


Figure 9 Path A represents the data stream where the flat fielding is done natively within NASA’s EXOTIC pipeline. Whereas path B represents the data stream when the flat fielding is done outside of the EXOTIC pipeline and then fed into EXOTIC for derivation of the light curve.

The flat fielding performed on path B is done in the nearly same way as described in section 2.2.1, the only difference is that the images from the CCD are pedestaled. Pedestalizing is when there is a small quantity of light, in this case the pedestal corresponded to 100 ADU (analog to digital units), ensure that pixels have a positive value. To avoid this pedestal, it needs to be removed, to do this the pedestal value is subtracted off of each pixel in the flats then processing to create the master flat can begin. Once the master flat has been created the pedestal is added back on since the images of the targets have this pedestal so it would be wrong to ignore it in the flat fielding of the target images.

The flat fielding process within the EXOTIC software is not exactly known; however, it is rational to assume that it follows nearly the same process as outlined in section 2.2.1. Once the

data has been flat fielded it can be entered back into EXOTIC to perform the light curve fit. After the fit is complete for both paths the residuals, midpoints, ratio of radii, and their respective uncertainties can be compared, and the validity of the claims made in section 2.2.5 can be substantiated or not.

3. Results

3.1 Overview of Results

Overall, there was a large spread in the success of EXOTIC in determining the midpoint and the ratio of radii. The alternate flat-fielding routine discussed in section 2.2.6 did not show consistent success at reducing the residuals. In some data sets EXOTIC was able to better minimize the residuals and in others the alternate flat-fielding routine was able to better able to minimize the residuals. Figures 10 and 11 show the results of a successful fitting routine, and the change in residuals from different flat-fielding methods.

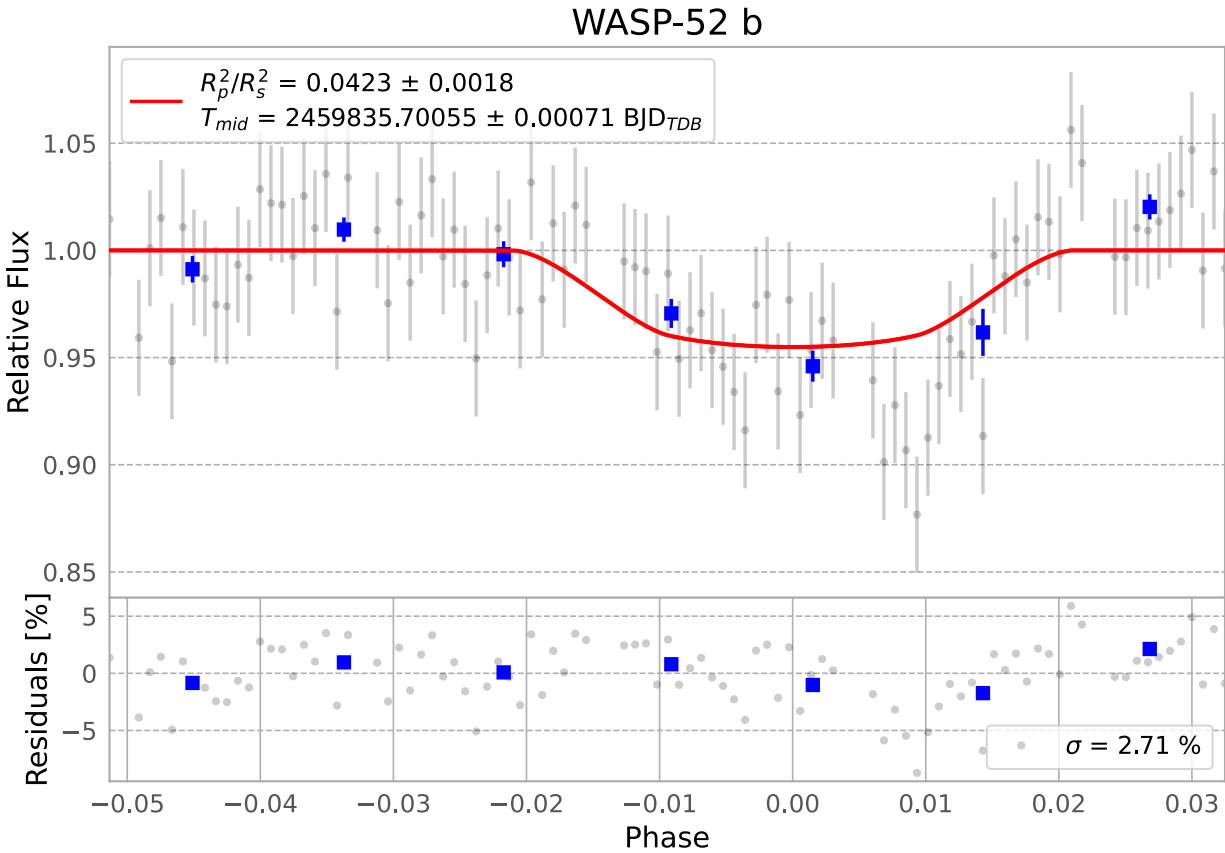


Figure 10 The final results of the EXOTIC fitting routine for the target exoplanet WASP-52b and star WASP-52. All data processing was done within the EXOTIC software. The R_p^2/R_s^2 value corresponds to the transit depth, the T_{mid} value corresponds to the exact time of specific transits midpoint, and σ value corresponds to the residuals.

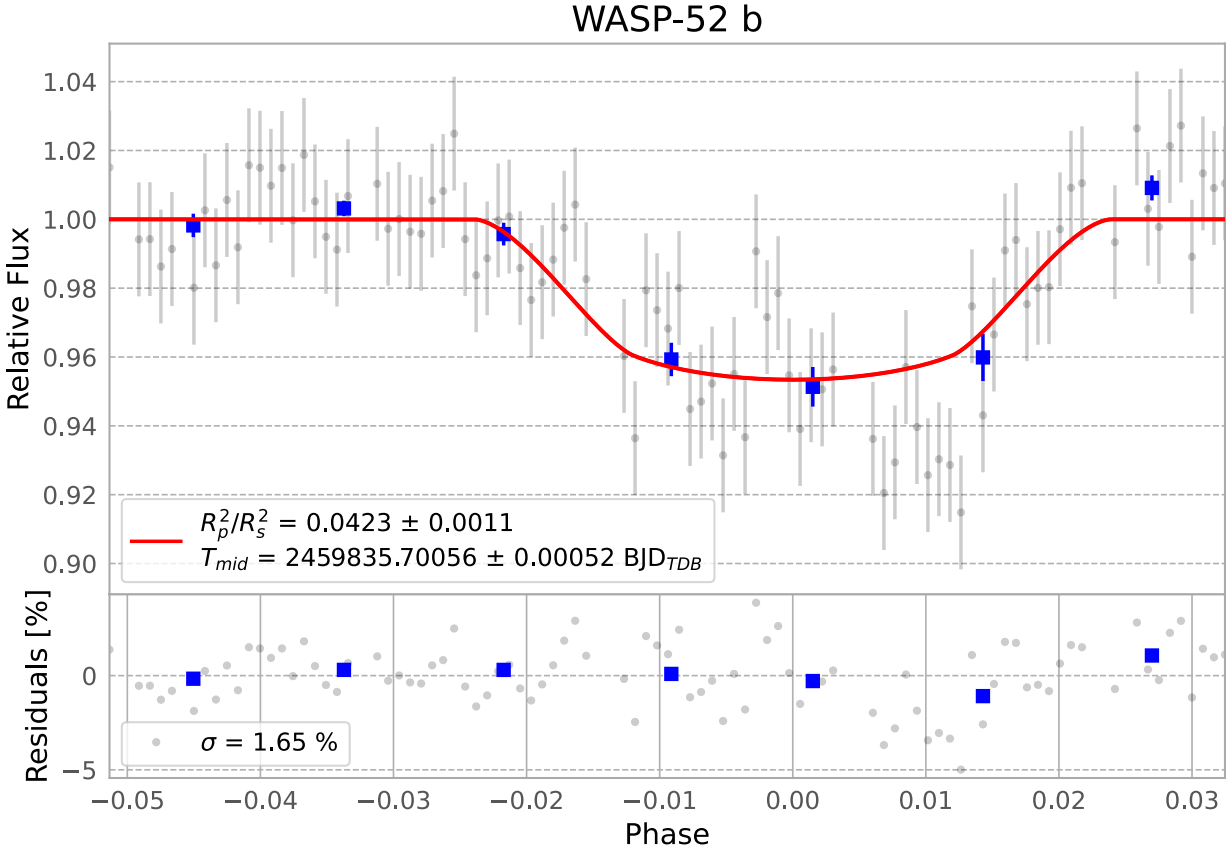


Figure 11 The final results of the EXOTIC fitting routine for the target exoplanet WASP-52b and star WASP-52. Flat fielding was done outside of EXOTIC the rest of the data processing was done within the EXOTIC software. The R_p^2/R_s^2 value corresponds to the transit depth, the T_{mid} value corresponds to the exact time of specific transits midpoint, and σ value corresponds to the residuals.

3.2 Residuals and Transit Midpoints

Table 1 shows the residuals for the five transits that were able to be processed by EXOTIC. The residuals are calculated by dividing each data point by the value of the model at that point, and then subtracting one. As can be seen Qatar-1 and Qatar-10 both have high residuals. These high residuals affected the downstream numbers, the lower the residuals the smaller the uncertainty and the closer values were to calculated values.

	Planet Observed				
	HD 189733	Wasp-52	Wasp-10	Qatar-1	Qatar-10
Star Flux Residuals	1.01%	2.71%	2.51%	31.96%	33.31%
Star Flux Residuals**	1.19%	1.65%	1.26%	33.07%	11.68%
Transit Depth	0.02250 +/- 0.00002	0.027093 +/- 0.000001	0.0292068 +/- 0.0000003	0.02372986200 +/- 5E-11	0.0193099930000 +/- 3E-13

Table 1 The cells highlighted in red have high residuals resulting in high uncertainties and less accurate results. The “***” represents that the cells in that row were calculated with the alternate data stream from 2.2.6. Note the transit depths, these are on the order of a couple percent. Since the residuals are the uncertainties represented on the final light curves, minimizing them so that they do not drown out the transits depths is important.

Since the residuals are a good way to estimate the accuracy of the results it comes as no surprise that the other values calculated are closer to the known values when the residuals are lower. As discussed in section 2 the midpoints are important in calculating the period and future transits. The midpoints for WASP-10, Qatar-1, and Qatar-10 were outside of the expected midpoint times, table 2 shows the midpoint times. Both Qatar-1 and Qatar-10 had high residuals and thus were not able to provide precise enough data to fit the correct midpoint time. This was not the issue for WASP-10, instead some of the data before the transit began had to be discarded so only the middle and end of the transit was fitted, see figure 11. In Wasp-10’s case the midpoint time was the only thing affected as the low residuals would imply.

	Planet Observed				
	HD 189733	Wasp-52	Wasp-10	Qatar-1	Qatar-10
Transit Midpoint (BJD-TDE)	2459823.665 +/- 0.002	2459835.7006 +/- 0.0007	2459850.58 +/- 0.02	2459829.602 +/- 0.003	2459870.22 +/- 0.07
Transit Midpoint** (BJD-TDE)	2459823.665 +/- 0.004	2459835.7006 +/- 0.0005	2459850.58 +/- 0.02	2459829.610 +/- 0.003	2459870.22 +/- 0.07
%Diff	7.72413E-08	4.06515E-10	0	3.00834E-07	8.13051E-08

Table 2 The cells highlighted in red, and blue had midpoints that were outside of the expected midpoints. The blue cell: however, was not a complete transit so the midpoint calculation was assigned by EXOTIC, the reason for the 0% difference. The “***” represents that the cells in that row were calculated with the alternate data stream from 2.2.6.

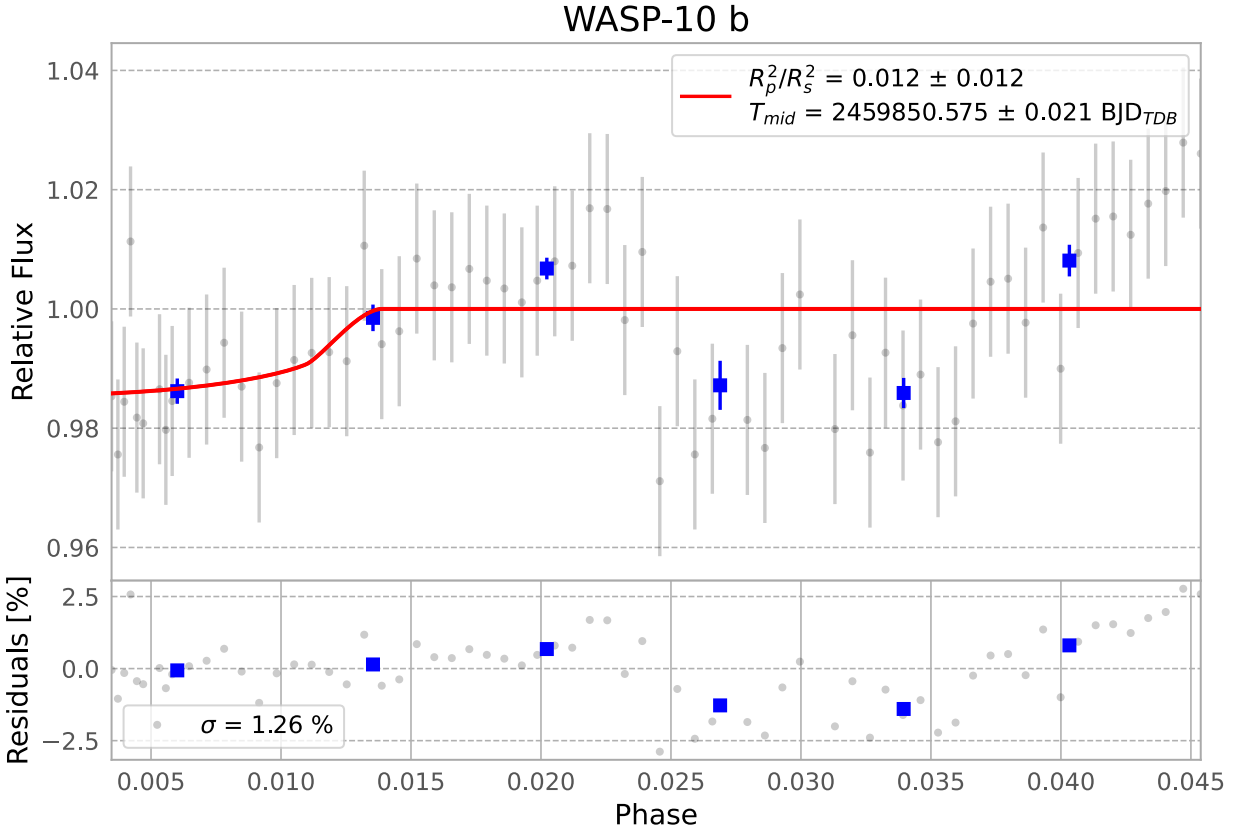


Figure 12 The final results of the EXOTIC fitting routine are shown for target exoplanet WASP-10b and star WASP-10. Flat fielding was done outside of EXOTIC the rest of the data processing was done within the EXOTIC software. The beginning parts of the transit were cut out resulting in the incomplete looking plot.

3.3 Ratio of Exoplanet Radius to Stellar Radius

The ratio of exoplanet radius to stellar radius is useful for a number of calculations, but for the purposes of this research it can be used to help confirm that a transit was actually observed. The depth of the transit can be found by taking the square of the ratio: $(\frac{R_p}{R_s})^2$. Table 3 shows the ratios of the previously discussed targets. Following the trend, the uncertainties are lower when the residuals are lower; however, the R_p/R_s values do not always agree with the known values whether or not the residuals are high.

	Planet Observed				
	HD 189733	Wasp-52	Wasp-10	Qatar-1	Qatar-10
Observed Rp/Rs	0.133 +/- 0.02	0.206 +/- 0.004	0.16 +/- 0.06	0.00 +/- 0.05	0.17 +/- 0.05
Observed Rp/Rs**	0.119 +/- 0.04	0.206 +/- 0.003	0.11 +/- 0.06	0.16 +/- 0.05	0.17 +/- 0.05
Known Rp/Rs	0.150 +/- 0.004	0.1646 +/- 0.0012	0.1709 +/- 0.0005	0.154045 +/- 0.000007	0.1389604 +/- 0.0000005

Table 3 From left to right, the first 3 columns of results have lower uncertainties with respect to their values. The “***” represents that the cells in that row were calculated with the alternate data stream from 2.2.6. Stassum [15] provided the known results.

3.4 Exoplanet Periods

The periods of the exoplanets were calculated from the semi-major axis over the stellar radius, a/R_s . Taking the semi-major axis out of this value, using stellar radius values from Stassun et al., the period can be calculated using the following equation:

$$T = \sqrt{\frac{a^3}{M_s}} \quad (2)$$

where T is the period, and M_s is the solar mass of the star the exoplanet orbits [15][16]. The periods found had uncertainties that were much larger than the uncertainties of the known periods. Four of the five targets had periods that agreed with the known values, see table 4 for the complete list of results.

	Planet Observed				
	HD 189733	Wasp-52	Wasp-10	Qatar-1	Qatar-10
Observed Period (days)	2.6 +/- 0.5	2.2 +/- 0.3	3.2 +/- 0.8	1.1 +/- 0.5	2.7 +/- 0.6
Observed Period** (days)	2.9 +/- 0.7	1.9 +/- 0.3	3.6 +/- 0.8	2.2 +/- 0.7	2.6 +/- 0.6
Know Period (days)	2.21857514 +/- 6e-08	1.7497808 +/- 0.0000004	3.0927289 +/- 0.0000007	1.42002433 +/- 3e-08	1.645320 +/- 0.000007

Table 4 All the planets observed have periods that agree with the known except Qatar-10. The “***” represents that the cells in that row were calculated with the alternate data stream from 2.2.6. Stassum [15] provided the known results.

4. Conclusion

4.1 EXOTIC Flat Fielding vs. Pre-Flat Fielding

There was no consistent advantage to be found when flat fielding images outside of the EXOTIC pipeline. Results showed that the residuals reduced for only some of the targets when flat-fielded outside of EXOTIC. Low residuals did result in a smaller uncertainties and more precise calculations as a result of the fit. Going forward it would be recommended to run the EXOTIC software with both flat fielded images and non-flat fielded images then select the output with the lower residuals.

4.2 Midpoints and Radii Ratio

Two of the five, HD 189733 and WASP-52, midpoints were within range of the expected values provided by the NASA Exoplanet Archive [17]. Of the three that were outside of the range of the expected values one, WASP-10, was an incomplete image set so the whole transit was not observed making it difficult for EXOTIC to calculate the correct midpoint. The two other transits, Qatar-1 and Qatar-10, were not able to be accurately fit resulting in out-of-range midpoints. This again implies the importance of reducing the residuals of image sets.

Of the five transits the three with the lowest residuals, HD 189733, WASP-52, and WASP-10, did not have a radii ratio that was within the range expected [17]. The two with the highest residuals, Qatar-1 and Qatar-10, were the only that had radii ratios within the expected range [17]. This fact seemingly counters the claim that the output with the lowest residuals should be selected; however, the uncertainties for the Qatar-1 and Qatar-10 were so large that the values

reported are not significant. For the first three transits, while the ratios do not fall within the expected range, they do suggest that a transit was observed.

4.3 Exoplanet Orbital Periods

Four of the five transits, HD 189733, WASP-10, WASP-52, and Qatar-1, have periods within the range expected as provided by the NASA Exoplanet Archive [17]. Even though periods are within the expected range, the measured uncertainties of all the periods are much larger than the known uncertainties. Additionally, Qatar-1 has uncertainties that are similar to other transits; however, due to its high residuals and inaccurate midpoint and R_s/R_p its period cannot be attributed to the data but to the expected values.

4.4 Future Works

The research done during this thesis can be continued in a variety of ways. Interesting research would be further investigating how to minimize the residuals and why EXOTIC performs better than external code for some data set and worse for others. Another avenue would be looking back at the same targets and making additional observations. The goal would be to refine the results of this research. Lastly, continuing to make observations with the overall goal of reducing the uncertainties would benefit any future observations.

References

- [1] *Your Guide to Exoplanets*. (n.d.). The Planetary Society.
<https://www.planetary.org/worlds/exoplanets>
- [2] Wolszczan, A., & Frail, D. A. (1992). A planetary system around the millisecond pulsar PSR1257 + 12. *Nature*, 355(6356), 145–147. <https://doi.org/10.1038/355145a0>
- [3] Borucki, W., & Koch, D. (2011). Characteristics of Planetary Candidates Observed by Kepler. II. Analysis of the First Four Months of Data. *The Astrophysical Journal*, 736(1).
<https://doi.org/10.1088/0004-637X/736/1/19>
- [4] Howell, S. B., Sobeck, C., Haas, M., Still, M., Barclay, T., Mullally, F., Troeltzsch, J., Aigrain, S., Bryson, S. T., Caldwell, D., Chaplin, W. J., Cochran, W. D., Huber, D., Marcy, G. W., Miglio, A., Najita, J. R., Smith, M., Twicken, J. D., & Fortney, J. J. (2014). The K2 Mission: Characterization and Early Results. *Publications of the Astronomical Society of the Pacific*, 126(938), 398–408. <https://doi.org/10.1086/676406>
- [5] SPIE. (2014). George R. Ricker plenary: Transiting Exoplanet Survey Satellite (TESS). *SPIE Newsroom*. <https://doi.org/10.1117/2.3201407.18>
- [6] Howell, S. B. (2020). The Grand Challenges of Exoplanets. *Frontiers in Astronomy and Space Sciences*, 7. <https://doi.org/10.3389/fspas.2020.00010>
- [7] Mayor, M., & Queloz, D. (1995). A Jupiter-mass companion to a solar-type star. *Nature*, 378(6555), 355–359. <https://doi.org/10.1038/378355a0>
- [8] Howell, S. B., Scott, N. J., Matson, R. A., Horch, E. P., & Stephens, A. (2019). High-resolution Imaging Transit Photometry of Kepler-13AB. *The Astronomical Journal*, 158(3), 113. <https://doi.org/10.3847/1538-3881/ab2f7b>

- [9] Zellem, R. T., Pearson, K. A., Blaser, E., Fowler, M., Ciardi, D. R., Biferno, A., Massey, B., Marchis, F., Baer, R., Ball, C., Chasin, M., Conley, M., Dixon, S., Fletcher, E., Hernandez, S., Nair, S., Perian, Q., Sienkiewicz, F., Tock, K., & Vijayakumar, V. (2020). Utilizing Small Telescopes Operated by Citizen Scientists for Transiting Exoplanet Follow-up. *Publications of the Astronomical Society of the Pacific*, 132(1011), 054401. <https://doi.org/10.1088/1538-3873/ab7ee7>
- [10] *Plan exoplanet transit observations*. (n.d.). Astro.swarthmore.edu. <https://astro.swarthmore.edu/transits/transits.cgi>
- [11] Meade 12" f/10 LX200 ACF Telescope with Giant Field Tripod. (2020). Meade.com. <https://www.meade.com/meade-12-f-10-lx200-acf-telescope-with-giant-field-tripod.pdp>
- [12] *Charged-Coupled Devices*. (n.d.). Retrieved April 25, 2023, from <http://scipp.ucsc.edu/~tesla/lecture2.pdf>.
- [13] Howell, S. B. (2006). Characterization of charge-coupled devices. *Handbook of CCD astronomy*. Cambridge University Press.
- [14] Blaser, E., Iturralde, A., & Smith, M. (n.d.). *How EXOTIC Works*. <https://github.com/rzellem/EXOTIC>
- [15] Stassun, K. G., Oelkers, R. J., Paegert, M., Torres, G., Pepper, J., Lee, N. D., Collins, K., Latham, D. W., Muirhead, P. S., Chittidi, J., Rojas-Ayala, B., Fleming, S. W., Rose, M. E., Tenenbaum, P., Ting, E. B., Kane, S. R., Barclay, T., Bean, J. L., Brassuer, C. E., & Charbonneau, D. (2019). The Revised TESS Input Catalog and Candidate Target List. *The Astronomical Journal*, 158(4), 138. <https://doi.org/10.3847/1538-3881/ab3467>
- [16] Nave, R. (2018). *Kepler's Laws*. Gsu.edu. <http://hyperphysics.phyastr.gsu.edu/hbase/kepler.html>

[17] *NASA Exoplanet Archive*. (2019). Caltech.edu. <https://exoplanetarchive.ipac.caltech.edu/>